Ingo Schewe · Thomas Soltwedel

Benthic response to ice-edge-induced particle flux in the Arctic Ocean

Abstract With the aims of investigating the response of the smallest benthic biota to a strong ice-edge-related input of phytodetritus, and of registering supposed lateral transportation processes of phytodetrital matter with northerly direction under the ice, we analysed a number of abiotic and biotic parameters in surface sediments from the northern Fram Strait. Two transects of 14 stations in total were made. One transect, crossing the Fram Strait from the east to the west, followed mainly the ice edge. The second transect extended latitudinally in a northerly direction, starting in ice-free areas, passing the ice edge, and ending in heavy ice-covered areas, approximately 100 nm north of the ice edge. Stations along this transect were sampled at almost constant water depths to avoid depth-related influences in our investigations. Results showed the expected high phytodetritus concentrations in the ice-edge vicinity. Concentrations of sediment-bound plant pigments were approximately 5 times higher than in ice-covered areas, indicating a very strong phytodetritus input. With increasing distance from the highly productive areas at the ice edge, we found significantly decreasing concentrations of phytodetrital input to the seafloor in a northerly direction. Within the foraminiferans, generic diversity was clearly reduced in the area of strong phytodetritus deposition. Along the latitudinal transect, out of the direct ice-edge influence, foraminiferal diversities slowly increased within increasing distance from the ice edge. The integration of results from earlier foraminiferal investigations, from stations further to the north, indicates a once more decreasing diversity with continually decreasing food supply.

I. Schewe (✉) · T. Soltwedel
Alfred-Wegener-Institut for Polar and Marine Research, Columbusstraße, Postfach 120161, 27568 Bremerhaven, Germany
E-mail: ISchewe@awi-bremerhaven.de
Fax: +49-471-48311776

Introduction

In the marginal seas of the Arctic Ocean, phytoplankton production is constrained by the strong seasonality in light and ice coverage. In early spring, light attenuation by the snow-covered ice sheet inhibits phytoplankton growth. Microalgal production starts with the development of ice algae in the bottom centimetres of the ice in response to the vernal increase in irradiance (Cota et al. 1991). This pre-bloom phase is characterized by ice algae and minute standing stocks, which grow slowly in a shade-adapted state under the ice. These stocks may form the basis for a rapid increase in biomass. The exponential growth phase begins when the ice breaks up and melts (Sakshaug and Skjoldal 1989). The bloom is typically short and hectic and constitutes a large fraction of the annual production, which ranges in the Arctic seas from 10 to 100 gC m^{-2} (Subba Rao and Platt 1984). At the ice edge, up to 70% of the phytoplankton stock may sink towards the bottom. Typically, the band of elevated primary production sweeps across the area of seasonal ice cover as the ice-edge bloom trails the retreating ice (Sakshaug and Skjoldal 1989).

Benthic communities in the Arctic experience low food input for most of the year. Episodic strong food pulses may act like "disturbances", favouring opportunistic species that can rapidly utilize high amounts of detritus. Since the first direct observation of rapid accumulations of phytodetritus on the deep seafloor, various studies have shown that benthic Foraminifera play an important role in the uptake and cycling of organic matter deposited in strong pulses (Altenbach 1992; Gooday et al. 1996).

A major question of benthic research in Arctic regions is: which are the pathways providing the benthos with particulate organic matter (POM). In this context, lateral transportation processes are supposed to be very important. The northern Fram Strait, located between Greenland and Svålbard, is well suited for studying how strong food pulses and a lateral transportation of POM affect the benthic environment. This region is charac-

terized by large annual fluctuations in ice-coverage, and large amounts of relatively warm and nutrient-rich Atlantic water flowing into the Arctic Ocean within the West Spitzbergen current (WSC) (Manley 1995; Rudels et al. 2000). Against this background, we visited in summer 1999, the marginal ice zone (MIZ) of the Fram Strait: (1) to follow the current-driven extent of ice-edge blooms in a northerly direction and to decipher the effect of decreasing phytodetritus availability on the benthic biota; (2) to study the effects of ice-edge induced phytodetritus pulses on the smallest benthic biota immediately in the bloom area, with special attention given to the foraminiferal diversity.

Materials and methods

Area of investigation

The Fram Strait is the only deep connection between the Atlantic and the Arctic Oceans. Located between Eastern Greenland and Svålbard (Fig. 1a), this region has central relevance for global water-mass exchanges. While one part of the sampling was done by crossing this passage at approximately 80°N, we also sampled a transect of stations located along the western flank of the Yermak Plateau between 79.5°N and 81.5°N.

The Fram Strait is characterized by an extensive water-mass exchange between the Greenland Sea and the Central Arctic Basins (Fig. 1a). Relatively warm and nutrient-rich Atlantic Water (AW) is transported within the West Spitzbergen Current into the central Arctic Ocean (Manley 1995). The WSC separates into two branches. The main inflow of Atlantic Water into the Arctic Ocean follows the Svålbard continental slope eastwards (Spitzbergen Branch, SB). A second branch, the Yermak Branch (YB), follows the bathymetry of the Yermak Plateau (Manley 1995; Rudels et al. 2000). This branch does not progress into the interior of the Arctic Ocean and is most likely recirculated back to the south at the western flank of the Yermak Plateau.

In the western part of the Fram Strait, approximately 75% of the total Arctic Ocean water outflow is transported in a southerly direction within the East Greenland Current (EGC) (Murray 1998). These surface waters transport large amounts of sea ice formed in the Arctic Mediterranean, keeping the eastern Greenland coast ice-covered all year-round, whereas the eastern part of the Fram Strait is generally ice-free during summer months (Fig. 1a).

The bioproduction in the area of investigation is directly coupled to these conditions. In the eastern Fram Strait, a high primary production in the MIZ supplies the benthos in the summertime with high amounts of "fresh" particulate detritus, which is partly transported in a northerly direction under the ice within the WSC. Ice-edge-related phytodetritus in the western Fram Strait is transported by the EGC in a southerly direction into ice-free regions of the NW Greenland Sea. Satellite-derived data from passive microwave sensors (DMSP-SSM/I, Kaleschke et al. 2001) showed only low wind-induced movements of the ice edge during the summer months July and August in 1999 (~20 nm). During the sampling period, the ice-edge position was almost constant.

Benthos sampling

Sediments were sampled in summer 1999 during the expedition ARK-XV/2 with the German research ice-breaker Polarstern. A total of 14 stations were visited (Table 1, Fig. 1b). Seven stations were located along a transect crossing the Fram Strait at approximately 80°N (transect-A). Another transect of eight stations in a northerly direction followed the western flank of the Yermak Plateau at about 1,000 m water depth (transect-B). This transect,
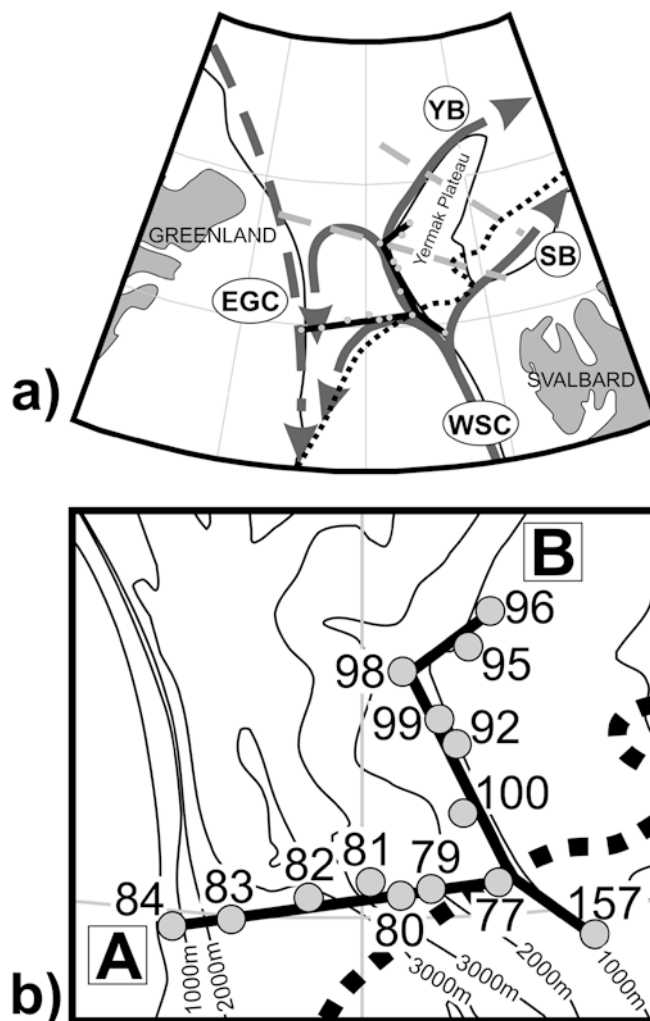

Fig. 1 a Fram Strait with main directions of currents transporting Atlantic and Arctic waters, after Rudels et al. (2000): West Spitzbergen Current (*WSC*), Spitzbergen Branch (*SB*) and Yermak Branch (*YB*), East Greenland Current (*EGC*) (*dotted black line* ice edge during ARK XV/2; *dotted light-grey line* 1997 sampled transects). **b** Enlargement of the sampling site with transects-A and -B

covering a distance of approximately 130 nm, started in open waters, crossed the ice edge and continued 100 nm in a northerly direction into the pack ice.

Virtually undisturbed samples were taken using a multicorer (MUC, Barnett et al. 1984). Due to limitations in ship time, generally only one MUC haul was performed per sampling site. Sediment cores were subsampled soon after recovery using plastic syringes with cut-off anterior ends (5 ml and 20 ml). The subcores were sliced into 1-cm-thick sections down to 5 cm depth, resulting in single sediment volumes of 1.17 cm^3 and 3.24 cm^3. Generally, three "pseudo"-replicates (Venrick 1971) from different MUC tubes of one haul were taken for each parameter investigated. To avoid distortions in the analysis of selected biochemical parameters, immediate processing directly onboard was necessary. All remaining subsamples were either fixated or deep-frozen for later investigations in the home laboratory.

Chloroplastic pigment equivalents (CPE)

The flux of phytodetritus to the seafloor was estimated by fluorometric determinations of sediment-bound chloroplastic pigments.

Table 1 Station data and environmental parameters: chlorophyll a (*Chl a*); Chloroplastic Pigment Equivalents (*CPE*)

	Station	Latitude	Longitude	Date	Water depth (m)	Ice-edge distance (nm)	Ice coverage (%)	Chl a ($\mu g \cdot cm^{-3}$)	CPE ($\mu g \cdot cm^{-3}$)
Transect-A	PS55/077	80°09′N	3°49′E	26.07.99	1475	0	20	0.95	6.58
	PS55/079	80°08′N	1°58′E	26.07.99	2177	14	80	0.48	4.10
	PS55/080	80°07′N	1°05′E	27.07.99	2850	21	50	0.49	3.88
	PS55/081	80°11′N	0°14′E	27.07.99	3020	34	90	0.63	3.14
	PS55/082	80°06′N	1°28′W	27.07.99	2845	50	80	0.40	2.42
	PS55/083	79°58′N	3°33′W	27.07.99	2345	72	70	0.01	0.83
	PS55/084	79°55′N	5°08′W	28.07.99	1131	120	70	0.03	1.33
Transect-B	PS55/157	79°52′N	5°59′E	31.08.99	1013	−29	0	0.62	4.94
	PS55/077	80°09′N	3°49′E	26.07.99	1475	0	20	0.95	6.58
	PS55/100	80°29′N	2°57′E	10.08.99	1486	22	90	0.20	3.27
	PS55/092	80°49′N	2°51′E	07.08.99	980	42	95	0.21	3.22
	PS55/099	80°54′N	2°28′E	10.08.99	1050	48	100	0.30	4.22
	PS55/098	81°10′N	1°15′E	09.08.99	1662	69	100	0.03	2.12
	PS55/095	81°16′N	3°22′E	08.08.99	750	89	100	0.07	2.64
	PS55/096	81°26′N	4°03′E	08.08.99	744	100	100	0.18	3.46

The bulk pigments registered by this method were termed chloroplastic pigment equivalents (CPE) (Thiel 1978).

Bacterial enumeration and biomass determination

Abundance and biomass of sediment-inhabiting bacteria were determined from each station. A single subcore with a diameter of 1.17 cm was sliced in 1-cm horizons and fixated in 2% formalin. In the home laboratory, after staining with acridine orange, bacterial cells were enumerated by epifluorescence microscopy using a wavelength of 450–490 nm. Calculated abundance of each value represents the mean of 40 grid counts of a single filtered sediment subsample. Bacterial volumes were determined with the New Porton Grid, measuring randomly 60 bacterial cells per filter (Grossmann and Reichhardt 1991). Bacterial biomass was finally calculated from determined volumes using the conversion factor 3.0×10^{-13} g C μm^{-3} given by Børsheim et al. (1990).

Bacterial exoenzymatic activities

Exoenzymatic esterase turnover rates were determined using the fluorogenic substrate, fluoresceine-di-acetate (FDA). The method, developed by Meyer-Reil and Köster (1992), determines the hydrolytic activity of organisms particularly involved in the primary decomposition of organic matter. To prevent loss in activity during storage, it was necessary to perform FDA determinations immediately after subsampling.

Investigations on benthic meiofauna

For meiofauna investigations, three subsamples (20-ml syringes), covering a total sediment surface of ~10 cm^2, were sectioned into single 3.24-cm^3 horizons and fixated in 4% formalin. Before sorting under a low-power stereo microscope, single meiofauna subsamples were stained with rose bengal for at least 3–4 h and afterwards sieved wet through a series of meshes (500, 250, 125, 65, 32 μm). Each size fraction was sorted separately, and organisms were identified to the major taxa: Foraminifera, Nematoda and Harpacticoidea/nauplii. All other taxa occurring in minor quantities (Turbellaria, Gastrotricha, Kinorhyncha, Bivalvia, Polychaeta and Ostracoda) were pooled into one category classified as "Others". Special attention was paid to the foraminiferans, because these protozoans generally dominate deep-sea meiofauna communities, especially in Arctic deep-sea regions (Schewe and Soltwedel 1999; Schewe 2001). Foraminifera were classified into three morphological groups: Rhizopoda with calcareous shells (e.g. *Boliminidae*, *Polymorhinidae*), chitinous Rhizopoda (*Allogromiidae*), and agglu-

tinating Rhizopoda (e.g. *Hormosinidae*, *Saccaminidae*). Specimens were determined at least down to genus level. The limitations of rose-bengal staining are well known (Corliss and Emerson 1990). Therefore, the conservative approach of recognizing "stained" rather than "live" Foraminifera was adopted. Nevertheless, used with care, this method gives results reflecting the live population very accurately. Only those specimens in which the tests and stercomata (faecal pellets) had a fresh appearance, and at least some stained protoplasm was present, were counted (Gooday et al. 1995).

Total microbial biomasses

The "total microbial biomass" (TMB), comprising bacterial, nanofaunal and meiofaunal organisms in the sediment samples, was parameterized by two different methods. Total adenylates (TA = ATP + ADP + AMP) represent the amount of cytoplasma and, therefore, TA values are closely related to biovolume (Karl 1993). TA were converted into organic carbon equivalents by the factor 1,000, as defined by Boetius and Lochte (1996). To avoid aberration from real TA concentrations, analysis was carried out immediately after sediment sampling, following the instructions given by Greiser and Faubel (1988).

Phospholipids (PL) are specific components of cell membranes. Thus, concentrations of PL quantify cell surfaces, and therefore bacteria especially are naturally overemphasized (Rajendran et al. 1992). PL were determined following a modified method applied by Boetius and Lochte (1994). Phospholipid concentrations were converted to TMB in terms of organic carbon, applying a conversion factor of 100 μmol P (g C)$^{-1}$ (Findlay and Dobbs 1993).

Data analyses

Realizing the limitations of pseudoreplicate sampling from a single gear per station (Hurlbert 1984), statistical differences between stations or station groups were analysed by the *U*-test.

A Spearman rank-correlation matrix was performed to identify relationships between single parameters. Analysis of covariance (ANCOVA) was applied to compare Svålbard slope stations from transect-A with stations along two transects already sampled in 1997 by Soltwedel et al. (2000) slightly further to the north (Fig. 1a, hatched pale-grey lines).

Diversity analysis using a neutral model

Selected statistical indices were calculated for the foraminiferal component of the meiofauna. The Shannon-Wiener diversity index

(H') was used for comparisons with predictions given by a neutral model (EH') adapted by Caswell (1976) from the genetic model developed by Ewens (1972). Caswell's model constructs an ecological "neutral" community with the same number of species and individuals as the observed community, assuming certain community assembly rules (random births/deaths and random immigrations/emigrations), but without interactions between species. The great advantage of this method, compared with other diversity indices, is its relatively sample-size independent measure of diversity (Platt and Lambshead 1985). A computer program designed by Goldman and Lambshead (1989) implements this model and calculates for each investigated station the deviation statistic (V) by subtracting EH' from H', dividing the result by the standard deviation of EH'. If $V = 0$, the sample is deemed to have been derived from a "neutral" assemblage; values $V < -2$ or $V > 2$ apply for statistically significant deviations. Where V is greater or less than 0, the assemblage is not neutral, i.e. positive values result from excess equitability, negative values from excess dominance.

Results

Spatial variations in phytodetrital input

Lowest and highest concentrations of sediment-bound chloroplastic pigments were found at stations along transect-A (Fig. 2). Concentrations ranged from 0.014 ± 0.003 µg Chl a cm^{-3}, and 0.831 ± 0.175 µg CPE cm^{-3} on the West-Greenland slope (stat. 83) to 0.947 ± 0.428 µg Chl a cm^{-3}, 6.579 ± 1.311 µg CPE cm^{-3} at the ice edge (stat. 77) located on the Svålbard continental slope. On the Greenland slope, Chl a concentration at station 84 was almost 30 times lower than in comparable water depth off Svålbard (stat. 77). On the eastern part of the Fram Strait, we found a pronounced depth gradient, with decreasing CPE concentrations with increasing depth (Table 1).

Figure 3 demonstrates the clear decrease of sediment-bound pigments with increasing distance from the ice edge (and simultaneously increasing ice coverage) in a northerly direction along transect-B. After a strong
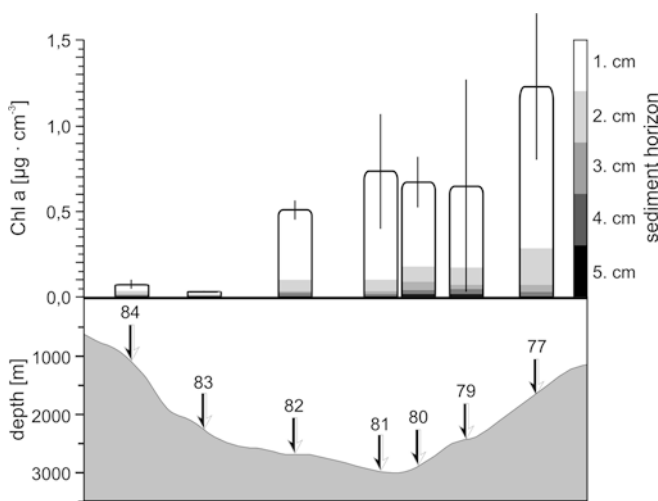

Fig. 3 Trends in concentrations of sediment-bound "fresh" plant pigments (Chl a) and foraminiferal diversities (Caswell's V), related to the ice-coverage along transect-B. *Unfilled triangles* and *circles* show results from 1997 investigations described in Soltwedel et al. (2000)

pigment peak occurring at station 77, concentrations decreased continuously down to 0.032 ± 0.003 µg Chl a cm^{-3}, 2.12 ± 0.381 µg CPE cm^{-3} at one of the northernmost stations (stat. 98). Pigment concentrations at station 77 were also almost 30% higher than on the ice-free station 157. At the ice-covered stations along transect-B, concentrations of intact Chl a were more than 2 times lower than in the deep Fram Strait (stat. 81), where Chl a values showed surprisingly high concentrations (0.632 ± 0.334 µg Chl a cm^{-3}).

Figure 4 exemplifies vertical gradients of CPE within the uppermost 5 cm of the sediment. The stations 77 and 95 were located at both ends of transect B. They represent two extremes in ice coverage and its influence on primary production. The differences between the sediment gradients of both stations are mainly developed by the high pigment concentrations at the sediment-water interface of ice-edge station 77. Whereas in the uppermost 2 cm of station 95, less than 50% of the total pigment concentration was present (integrated values over 5 cm = 100%), more than 60% of the pigments were detected in the upper 2 cm of station 77.

Bacterial standing stock and activity

Bacterial numbers at the sediment surface (0–1 cm) ranged between 4.7 and 13.7×10^8 cells cm^{-3}; bacterial biomass varied between 8.4 and 28.9 µg C cm^{-3} (Table 2). For pigments, highest and lowest values were found at the easternmost and westernmost stations of

Fig. 2 Chl a concentrations indicating "fresh" plant pigments in the uppermost 5 cm of the sediments at transect-A. Single sediment centimetres are characterized by different shadings of grey
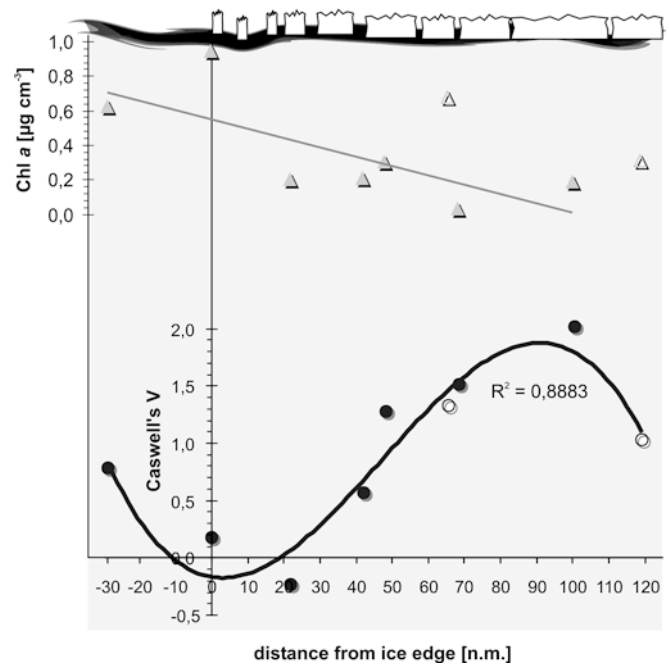
Fig. 4 Gradients of total plant pigments concentrations (*CPE*) in the upper 5 sediment cm of two selected stations from transect-B (*black* chlorophyll *a*, *grey* phaeopigments)
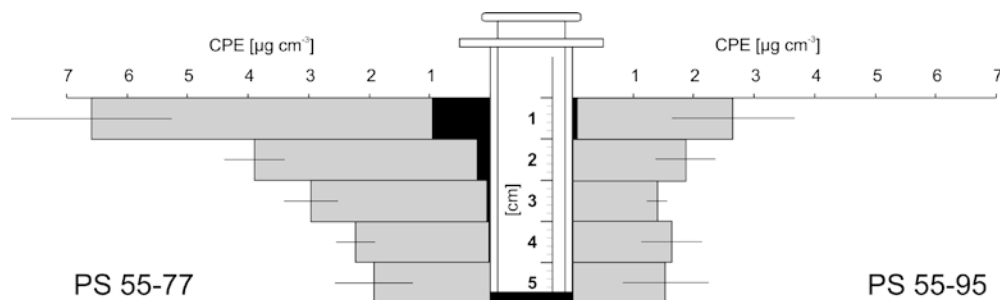

Table 2 Exoenzymatic hydrolytic activity (*FDA*) and bacterial abundance (*BN*), as well as various determined biomass parameters and their portion of the total microbial biomass (*TMB*, calculated from phospholipid concentrations) (*BB* bacterial biomass, *ADEN* TMB estimates from adenylates, *PLIPID* TMB estimates from phospholipids, *NB* nematode biomasses)

	Station	FDA (nmol/ml·h^{-1})	BN (10^8 cm^{-3})	BB (µgC·cm^{-3})	TMB	
					ADEN (µgC·cm^{-3})	PLIPID (µgC·cm^{-3})
Transect-A	PS55/077	2.70	13.65	28.87	62.72	167.65
	PS55/079	4.15	6.36	10.32	85.14	42.91
	PS55/080	1.43	8.43	15.74	67.00	20.51
	PS55/081	3.27	12.35	26.07	31.65	34.42
	PS55/082	3.45	10.58	23.43	16.85	41.68
	PS55/083	0.61	4.71	10.91	28.65	61.03
	PS55/084	0.74	4.71	8.38	30.74	26.39
Transect-B	PS55/157	2.01	9.69	17.67	46.89	35.31
	PS55/077	2.70	13.65	28.87	62.72	167.65
	PS55/100	1.95	10.76	15.20	40.56	43.47
	PS55/092	3.01	8.11	14.39	156.56	38.15
	PS55/099	3.05	8.39	14.59	67.92	89.74
	PS55/098	3.40	12.53	23.87	77.63	29.81
	PS55/095	2.76	10.58	17.73	89.52	52.31
	PS55/096	3.29	8.34	11.01	51.17	35.73

transect-A, with maximum values at the ice edge (stat. 77) and lowest values at the Greenland slope (stat. 84). Comparably high bacterial numbers and biomasses were found at the deepest station in the central Fram Strait (stat. 81; 320 m; 26.1 µg C cm^{-3}). Consequently, neither bacterial numbers nor bacterial biomasses showed a clear decrease with increasing water depth.

Bacterial exoenzymatic esterase activity neither showed a relationship to water depth, nor to bacterial numbers or biomasses (Table 2). Surprisingly, along transect-B, esterase activities generally increased in a northerly direction. Highest activities along this transect were found at station 96 (3.3 nmol cm^{-3} h^{-1}), whereas at the ice edge (stat. 77) the activity was slightly lower (2.7 nmol cm^{-3} h^{-1}). Overall lowest activities, however, were again found on the eastern Greenland slope (<1 nmol cm^{-3} h^{-1}).

Meiobenthic distribution patterns

Total meiobenthic abundances (including Foraminifera) at the sediment surface (0–1 cm, Table 3) ranged between 354 ± 56 and $1,743 \pm 507$ ind. 10 cm^{-2}. Amazingly, highest abundances were found at the deepest station in the central Fram Strait (stat. 81). Disregarding this particular station, meiofaunal abundances generally decreased with increasing water depth. Lowest meiofaunal abundances were found at station 100 (transect-B),

which is unusual compared with the altogether higher abundances in comparable water depths of neighbouring stations along this transect.

Foraminifera appeared to be the most dominant meiofaunal group, with an average proportion of $61 \pm 9\%$ at the sediment surface. Highest relative proportions were found at the deepest stations in the Fram Strait (up to 74% at stat. 81), whereas at shallower stations of transect-B, relative proportions of the Foraminifera sporadically decreased to less than 50%. Because of the group's dominance, it was chosen for further taxonomical investigations, with organisms determined down to genus level. Within all determined Foraminifera at the sediment surface (integrated over all stations), specimens of the calcareous genera *Epistominella* (508 ind. 10 cm^{-2}) and *Bolivina* (340 ind. 10 cm^{-2}) were most dominant. Within the agglutinating Foraminifera, specimens of the genus *Reophax* (221 ind. 10 cm^{-2}) were highly abundant, and the chitinous family *Allogromiidae* was dominated by *Nodellum* species (159 ind. 10 cm^{-2}). A comparison of the composition of morphotypes showed clear differences between transects-A and -B (Table 3). Along the Yermak Plateau (transect-B), the ratio of calcareous:agglutinating:chitinous Foraminifera was approximately 5:2:3. Crossing the Fram Strait (transect-A), the proportion of Foraminifera with calcareous shell clearly increased at the deep stations. Here the ratio was shifted to the debit of agglutinating and chitinous Foraminifera to 8:1:1.

Table 3 Summarized results of meiofaunal investigations from the uppermost sediment-centimetre. Total abundances of meiofauna (*total Meio*), as well as Foraminifera (*total Foram*). Proportions of the three morphological groups to the total foraminiferal abundances: *CHIT* chitinous shell, *AGGL* agglutinated shell, *CALC* calcareous shell. Diversity parameters calculated on genus level exclusively for the foraminiferans (*H'* Shannon-Wiener diversity, *EH'* Caswell's model diversity, *V* deviation from the model diversity related to the Shannon index)

	Station	total Meio (ind·10 cm^{-2})	total Foram (ind·10 cm^{-2})	Foraminifera					
				% CHIT	% AGGL	% CALC	$H'(\log_e)$	EH'	V
Transect-A	PS55/077	1320	734	26	24	50	1.96	1.92	0.19
	PS55/079	1074	754	11	8	81	1.86	1.55	1.18
	PS55/080	597	420	4	9	87	1.88	1.77	0.47
	PS55/081	1743	1291	7	4	88	1.55	1.57	−0.08
	PS55/082	601	426	15	5	80	1.71	1.67	0.16
	PS55/083	639	374	11	5	84	1.85	1.72	0.60
	PS55/084	810	474	14	11	75	1.90	1.55	1.46
Transect-B	PS55/157	1364	783	44	16	38	1.92	1.72	0.79
	PS55/077	1320	734	26	24	50	1.96	1.92	0.19
	PS55/100	354	160	41	23	36	1.79	1.83	−0.22
	PS55/092	814	480	39	29	33	1.93	1.80	0.58
	PS55/099	1066	711	14	17	68	2.16	1.87	1.29
	PS55/098	569	271	16	44	40	2.05	1.72	1.52
	PS55/095	929	606	28	23	49	2.07	1.82	1.10
	PS55/096	471	243	22	24	54	2.08	1.66	2.03

The metazoan meiofauna was dominated by Nematoda ($83 \pm 8\%$). Their relative proportion on the total meiofauna (including Foraminifera) was $33 \pm 8\%$ on average. Copepoda (Harpacticoidea + nauplii) were the third dominant group within the total meiobenthos and appeared with $4 \pm 2\%$. The bulk of all other taxa made up about $3 \pm 1\%$.

Examining the size structure of the meiobenthic community, determined by the fractionated wet-sieving method, we found at all stations that meiofaunal organisms of the smallest fraction ($> 32 \mu m$) were most abundant, occurring at $39 \pm 6\%$ on average, and a comparison of size compositions at stations of transect-A and transect-B showed no clear differences.

Statistical approaches to estimate foraminiferal diversity

Diversity patterns within the meiobenthic community were exclusively estimated for foraminiferans (Table 3). Statistical investigations were initiated by an analysis of similarities in foraminiferal taxon composition within the surface sediments (0–1 cm) of all sampled stations. This was done by a cluster analysis and a non-metric multidimensional scaling procedure (MDS). Figure 5a shows a dendrogram of all 14 stations, using group average clustering from Bray-Curtis similarities on square-root transformed abundances. Two groups of stations separated at the 72% similarity threshold combined stations of transect-A, and of transect-B, respectively. Further stepwise grouping within cluster-A probably reflects the influence of water depth as a strong environmental parameter for structuring the foraminiferal community.

Deviations (*V*) from Caswell's model-diversity are expressed in Fig. 5b by circles of various size. Here, stations of transect-B almost mirrored their geographical arrangement, with generally increasing positive *V* to the north. Within the transect-A cluster, deepest stations and stations located near the ice edge showed almost neutral *V*-values. Stations of transect-A showed generally low deviations from Caswell's model-diversity ($V < 0.7$), whereas ice-covered stations along transect-B generally showed deviations of $V > 1.0$, even increasing up to a significant level of $V \geq 2.0$ at the most northerly station 96.
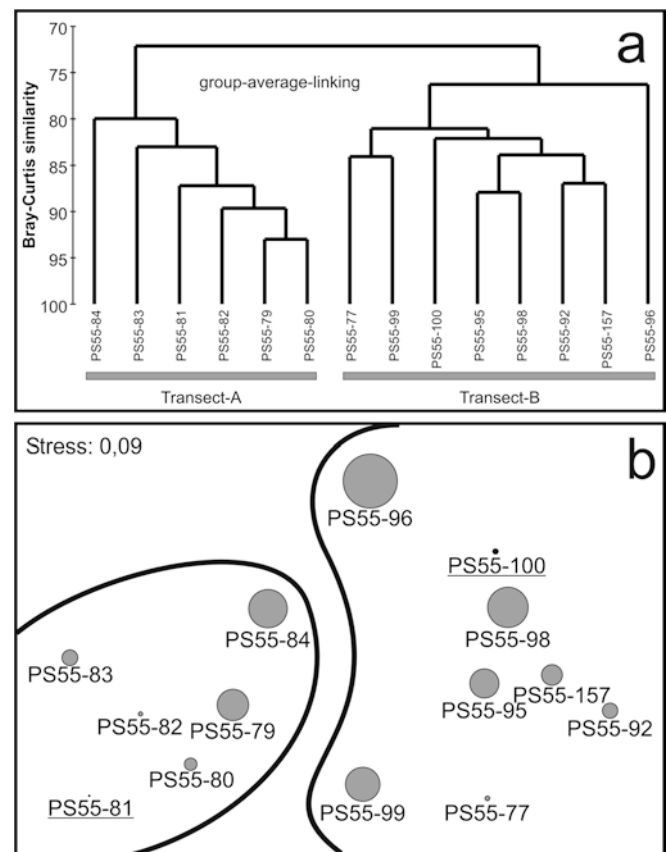

Fig. 5 a Dendrogram of the 14 investigated stations, using group average clustering from Bray-Curtis similarities on root-transformed standardized abundances. **b** Two-dimensional MDS configuration with superimposed dendrogram-clusters, at the similarity level of 72%. *Circle* sizes represent Caswell's *V*-values (*underlined* stations showing negative *V*)

Fig. 6 Spearman rank correlation matrix separately determined for both transects. (*DEPTH* water depth, *ICE* distance to the ice edge, *PHAEO* phaeopigments, *CHLA* chlorophyll *a*, *TMB* total microbial biomass (from phospholipids), *BB* bacterial biomass, *BN* bacterial numbers, *FDA* exoenzymatic hydrolytic activity, *META* metazoan meiofaunal, *FORAM* foraminiferal meiofaunal, *H'* Shannon-Wiener diversity, *V* deviation from Caswell's model-diversity). Levels of significance: *white* $P \le 0.05$; *grey* $P \le 0.01$; *black* $P \le 0.001$

Transect-B \ Transect-A	DEPTH	ICE	PHAEO	CHLA	TMB	BB	BN	FDA	META	FORAM	H'	V
DEPTH												
ICE			-8,140 p=0,00	-3,220 p=0,02								
PHAEO				3,721 p=0,01								
CHLA		-3,111 p=0,02	5,203 p=0,00				4,204 p=0,01					
TMB												
BB							5,996 p=0,00					-4,433 p=0,01
BN	2,500 p=0,05					5,203 p=0,00						-3,312 p=0,02
FDA		2,679 p=0,04										
META				3,111 p=0,02								
FORAM										7,650 p=0,00		
H'			3,377 p=0,01	-2,679 p=0,04				3,692 p=0,01				
V			2,679 p=0,04									

Parameters to estimate the total microbial biomass

Two non-specific parameters were used for the determination of the total microbial biomass: both total adenylates (TA) and phospholipids (PL) are commonly used indicators for "living biomass". Concentrations of TA and PL were finally converted to carbon equivalents.

Total microbial biomasses in the surface sediments (0–1 cm; Table 2) ranged from 16.9 to 156.6 µg C cm^{-3} from TA determinations, and from 20.5 to 167.64 µg C cm^{-3} from PL determinations, respectively, and thus showed a good agreement. However, related to water depth and distance from the ice edge, biomasses determined from TA and PL showed opposite gradients. While PL-biomasses decreased, TA-biomasses showed increasing values.

Correlations between determined parameters

A Spearman rank-correlation was performed with selected environmental parameters representing hydrostatic pressure, ice-coverage and food availability (i.e. water depth, distance from the ice edge and chloroplastic pigments), biochemically determined activity and biomass parameters (i.e. bacterial esterase activity = FDA and phospholipids = TMB), bacterial numbers/biomasses, as well as meiofaunal abundances and foraminiferal diversity parameters (*H'*, *V*). Correlation analyses were done for data from stations of transect-A and -B separately (Fig. 6). Sediment-bound plant pigments showed a good correlation with distance from the ice edge, but not with water depth. For both transects, Chl *a* concentrations, indicating "fresh" phytodetritus, significantly decreased with increasing distance from the ice edge ($P \le 0.05$). Phaeopigments (the bulk of pigment degradation products) showed this correlation at an even higher level of significance ($P \le 0.001$), however, only for transect-A. Significant positive correlations ($P \le 0.01$) between Chl *a* and phaeopigments on both transects, may indicate the relative freshness of the phytodetritus. Bacterial numbers correlated significantly ($P \le 0.01$) exclusively with Chl *a* for transect-A. For transect-B, Chl *a* significantly ($P \le 0.05$) correlated with metazoan abundances and foraminiferal diversity (*H'*). Bacterial biomass was the only biomass parameter showing any relationship with other parameters. For transect-A, a significant correlation ($P \le 0.01$) was found with low foraminiferal diversity. For the same transect, foraminiferal diversities also significantly correlated with bacterial abundances ($P \le 0.05$). For transect-B, exoenzymatic activities significantly correlated with increasing distance from the ice edge ($P \le 0.05$), as well as with foraminiferal diversity ($P \le 0.01$). For the same transect, both foraminiferal diversity-indices showed significant correlations with distance from the ice-edge (*H'*: $P \le 0.01$; *V*:$P \le 0.05$).

Discussion

The aim of this study was to investigate the influence of ice-edge-related enhanced primary production on the deep-sea benthos in a peripheral region of the Arctic

Ocean. We addressed two major questions on our investigations performed in the marginal ice zone of the Arctic Fram Strait: first, what distances can be covered by phytodetrital matter produced at the ice edge and laterally advected by the northwards-flowing currents, and how do benthic communities react to gradients in organic-matter supply associated with such transportation processes? Second, does ice-edge-related phytoplankton production and deposition, acting as a natural disturbance, affect the diversity of benthic communities?

Stations crossing the Fram Strait (transect-A) were sampled to investigate depth-related distribution patterns of the smallest benthic biota. The eastern part of this transect (stats. 77–81) almost followed the ice edge during the sampling campaign. Thus, these sites were areas of enhanced primary production and subsequent sedimentation of POM in relation to the ice edge. Transect-A also shows the southerly extension of investigations already carried out at the Yermak Plateau in 1997 (Soltwedel et al. 2000) almost 70 and 120 nm further to the north (Fig. 1a). Standardized methods and comparable ice conditions (position of the ice edge) during both sampling campaigns allow a direct comparison of data from the three transects. The importance of laterally transported organic matter as a food source for benthic organisms in ice-covered regions of the Arctic Ocean was already known and has been studied by several scientists (Boetius and Damm 1998; Walsh et al. 1998; Soltwedel et al. 2000). However, previous results were limited either by varying water depth of stations or by an insufficient number of sampling sites that could appropriately track a supposed lateral gradient. Sampling along transect-B was done to follow decreasing deposition rates of laterally transported phytodetritus by a high number of stations sampled in a northerly direction at almost constant water depths. The narrow row of stations allowed detailed investigations of the gradient in decreasing food availability and its influence on colonization by the deep-sea benthos.

Organic-matter supply to the benthos

Marginal ice zones belong to the most dynamic areas in the world's oceans, with large seasonal and inter-annual fluctuations in ice coverage and ice transport (Falk-Petersen et al. 2000). The pigment inventory bound in the sediment is a good indicator for estimating the input of phytodetritus to the seafloor. Within the area of investigation, ice coverage is the most relevant limiting factor for primary production during the Arctic summer. The onset of primary production is directly related to the seasonal availability of incident light and melting of the ice (Sakshaug and Slagstad 1991). Strong pulses in primary production are coupled to the spatial variation in ice cover, nutrient entry by Atlantic waters and the stratification of the water column due to melting processes. Ice melting during the Arctic spring and summer gives rise to a strongly stratified and nutrient-rich euphotic zone, with a distinct phytoplankton bloom. The phytoplankton blooms follow the receding ice edge as it melts during the spring and summer (Sakshaug and Skjoldal 1989) and intensive blooms occur in leads as the MIZ opens up. However, subjective observations, as well as sea-ice maps from passive microwave sensors (DMSP-SMM/I), suggest for the area of investigations an almost static position of the ice edge during July and August.

Assuming a close pelago-benthic coupling, sediments can mirror primary production within the euphotic zone affected by inhibiting and promoting factors, respectively. A peak in sediment-bound pigment concentrations close to the ice edge (stat. 77) indicates enhanced primary production in the MIZ. Strong regional differences in sediment-bound pigment concentrations on the eastern and western side of the Fram Strait (transect-A) demonstrate the combined effects of ice coverage and a current-driven transport of particles, including phytodetrital matter. The sedimentation of phytodetritus at stations in the central and eastern part of the Fram Strait (stats. 82–77) is influenced by the WSC. The overall low pigment concentrations at stations on the East Greenland slope (stats. 83 and 84) reflect generally low amounts of phytodetritus, transported by southward-flowing polar waters in the EGC.

Generally decreasing pigment concentrations with increasing water depth reflect gradual stages of degradation after vertical passing through the pelagic food-web (Billett et al. 1983). High amounts of intact plant pigments point at a relatively fast sedimentation and imperfect degradation in the pelagial. Rapid sedimentation of POM from primary production via "fluffy" aggregates was demonstrated for ice-free oceanic regions, e.g. for the NE Atlantic (Billett et al. 1983). Relatively high Chl a concentrations, especially in great water depths along transect-A (stats. 79–82), reflect the rapid sedimentation of aggregated phytodetritus created in the MIZ. Results from two transects already sampled in 1997 at 81 and 82°N crossing the Yermak Plateau slope, ~70 nm and ~120 nm north to the ice edge, showed continuously decreasing values with increasing water depth and, as expected, generally lower pigment concentrations (Soltwedel et al. 2000). This decrease in sediment-bound Chl a between transect-A (this study) and transects investigated in 1997 was statistically significant, as confirmed by analyses of covariance. The Fram Strait region, however, is well known for large inter-annual fluctuations in local ice coverage, and in the intensity of ice-edge blooms (Sakshaug and Skjoldal 1989), which makes a comparison of results from different years somewhat vulnerable. Therefore, in 1999, we carried out a quasi-synoptic sampling programme along a latitudinal transect between 79°N and 81.5°N. As expected, we found a highly significant ($P = 0.001$) decrease of Chl a, and a significant ($P < 0.05$) decrease in phaeopigments with increasing distance from the ice edge. This is attributed to the lateral advection and sedimentation of phytodetritus actually produced in
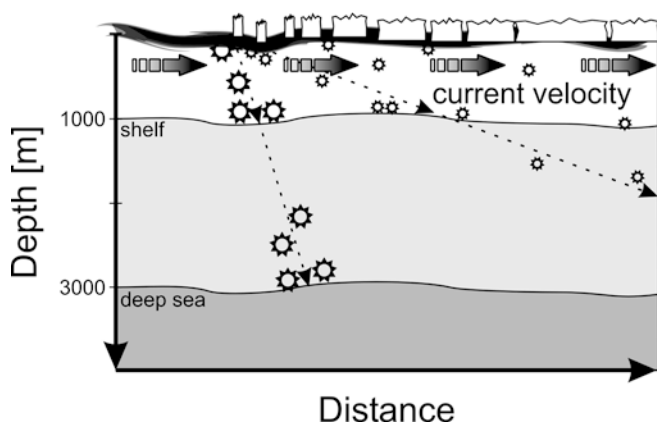
Fig. 7 Scheme for laterally transported detritus predominantly grown at the ice edge (*hatched arrows* vectors for sedimentation of heavy aggregated phytodetritus (*large stars*) as well as light phytodetritus particles (*small stars*))

summer 1999 at the ice edge. High Chl *a* concentrations found at the deep stations of transect-A, as well as the strong peak of sediment-bound Chl *a* at station 77, indicate the deposition of large amounts of relatively fresh POM produced at the nearby ice edge. Deep stations in the Fram Strait (stats. 80, 81, 82) showed, on average, 3 times higher concentrations of "fresh" plant pigments than at shallower stations along transect-B at a comparable distance to the ice edge (stats. 100, 92, 99). Figure 7 might help to clarify this apparent disproportion. The distance phytodetrital particles are laterally transported depends on several factors. Beside simple current velocities carrying the POM, particle mass, and especially the water depth, play an important role. "Heavy" particles will sink much faster than lighter ones. Furthermore, at great water depth, particles are able to sink for longer in a vertical direction, and consequently over longer distances, than on shallow-shelf areas. Thus, at the shallow transect-B, large aggregated phytodetritus particles reached the seafloor after a short phase of sedimentation. These particles can only be transported laterally for short distances from the ice edge in a northerly direction, resulting in the strong pigment peak found at station 77. Only phytodetritus with less mass is laterally transported over a long distance, and serves as a food source also in areas further to the north. This is indicated by the described northerly decreasing gradient of sediment-bound plant pigments. Also, the low CPE gradient within the sediment column of northernmost stations (Fig. 4) gives a good indication of generally reduced phytodetritus input in these permanently ice-covered areas.

At deep areas of transect-A, because of the great water depth, aggregated "heavy" phytodetritus particles stay for longer times in the water column. Thus, although these aggregates are comparably heavy, they can be transported laterally for longer distances and also reach locations with some distance to the ice edge. This might explain comparably large amounts of sediment-bound Chl *a* at stations up to 50 nm away from the ice edge (stat. 82).

Compared to pigment concentrations in central-Arctic sediments (Pfannkuche and Thiel 1987; Soltwedel and Schewe 1998), our investigations showed comparably high values. When extrapolating the latitudinal gradient of sediment-bound pigments, a lateral transport of POM covering an even greater distance into regions further to the north and not reached in this investigation, appeared to be possible.

Smallest benthic biota in relation to food availability

Strong sedimentation pulses in the eastern part of transect-A, indicated by comparably high concentrations of sediment-bound Chl *a*, obviously imply enhanced bacterial abundances in these sediments. However, it is not known whether part of the high bacterial standing stock originates from the pelagic realm and is deposited together with phytodetritus aggregates, or if those high abundances result from a strong offspring of sediment-inhabiting bacteria subsequent to an enhanced input of fresh organic matter. At the same stations in the deep Fram Strait, we also found comparably high foraminiferal abundances with simultaneously low biodiversities. The significant decrease of Caswell's diversity parameter *V* (coinciding with increasing bacterial biomasses and abundances) reflects a shift within the foraminiferal community towards excess dominance of single species. This shift is probably mainly caused by a large offspring of opportunistic foraminiferal species reacting to the pulsed deposition of large food quantities (Wollenburg and Kuhnt 2000). At station 81 especially, we found extremely high abundances of specimens from the genus *Epistominella*. *Epistominella exigua* and related species are regarded as typical opportunistic "phytodetritus species" (Gooday 1994; Smart and Gooday 1997).

Benthic investigations at stations along transect-B were performed to follow the effects of sedimenting phytodetritus, laterally transported by the WSC in a northerly direction. The decreasing deposition of phytodetritus with increasing distance from the ice edge was manifested by a continuous decrease of sediment-bound Chl *a* along the transect in a northerly direction. Effects of continuously decreasing food supply on the smallest benthic biota, however, were only found for a few investigated parameters, like exoenzymatic activities or metazoan abundances. All other parameters concerning the smallest benthic biota only showed some weak and non-significant trends. Phospholipid values, representing cell-wall compounds and thus organisms' surfaces, reflected a slightly decrease in TMB with increasing distance from the ice edge. At the same time, adenylates, indicating organisms' volumes, showed a slight increase in TMB along that transect. From this, we might speculate that the mean body size of organisms, covered by these biomass investigations, probably tends to get

larger with increasing distance from the ice edge, since larger organisms generally have a higher body volume and less surface than smaller organisms. However, neither bacterial volumes nor meiofaunal size-spectra showed a comparable trend. Adenylate concentrations in the sediments might also be influenced by increasing organism activities, as detected by increased esterase turnover rates.

We assumed a strong influence of ice-edge-related processes on the benthic community in the area of investigation. But simple determinations of organisms' abundance and biomass yielded no convincing results. This led to investigations on specific changes in the community structures of selected organism groups. Foraminifera, especially, were suitable subjects for investigations concerning organisms' diversity. They dominated the meiobenthic community with proportions of approximately 60%, and their short reproduction cycles enable rapid reactions to changing environmental conditions. A first examination of the morphological composition of foraminiferal assemblages explicitly showed higher proportions of calcareous Foraminifera at stations deeper than 2,000 m. At the deep stations of transect-A, the mean ratio of calcareous:agglutinating:chitinous Foraminifera was 8:1:1. Along transect-B, the relative proportion of calcareous Foraminifera was reduced, resulting in a mean ratio of 5:2:3. Similar proportions in the morphological composition already pointed to a generally higher diversity at generally shallower stations along transect-B. The significant coupling of enhanced extra-cellular enzymatic activity (FDA) and enhanced foraminiferal diversity pointed to a more effective food consumption of comparably diverse protozoan communities.

In order to asses the effect of "disturbance" on the foraminiferal community caused by strong pulses of phytodetritus deposition created at the ice edge, we used the Evens/Caswell model to detect deviations of real diversities from predicted neutral-model diversities (Platt and Lambshead 1985; Lambshead and Platt 1988). The results given by this model parameterization showed that diversities at investigated stations were generally higher or almost neutral, compared with the predicted model diversities. Lowest deviations from model diversities were found for transect-A, especially at the deepest stations, and also for transect-B at stations near the ice edge (≤ 40 nm). A common feature at these stations were high concentrations of sediment-bound Chl a. Figure 3 shows the significant increase ($P = 0.04$) of Caswell's V with increasing distance from the ice edge along transect-B, coincident with simultaneously decreasing CPE concentrations. At station 65, the real diversity (H') finally achieved a statistically significant deviation from the model diversity EH' ($V = 2.03$). The sketched polynomial function includes calculated diversities of two stations sampled at comparable water depth in 1997 (Soltwedel et al. 2000). The shape of this function is similar to typical curves of ecological succession as proposed by Connell (1978). According to his "intermediate disturbance hypothesis", ice-edge-related food pulses may act like "disturbances". On the assumption that the intrinsic diversity in the area of investigation is higher than a predicted model diversity (stat. 157), a "mild disturbance" would lead to almost neutral Caswell-diversity (e.g. stat. 77). The enhanced intrinsic diversity is caused by an excess equitability resulting from highly variable sedimentation of comparably fresh organic matter into the benthic system. With increasing distance from the ice edge, the frequency of a patchy phytodetritus sedimentation, and also the intensity (quantity) of the supply of fresh organic matter continuously decreases. Thus high foraminiferal diversity, far away from the ice edge, is not related to direct disturbance but probably to reduced growth rates, caused by the paucity of food laterally transported. Due to hunger stress at the northernmost investigated stations (e.g. stats. 98, 96), the population densities of the foraminiferans were clearly reduced. As for disturbances, Huston (1979) suggested that population growth rates might also have a similar effect on diversity. Connell (1978) noted that this is an extension of the intermediate disturbance hypothesis and should be true, other things being equal.

Returning to our hypothesis formulated earlier, we can now state that ice-edge-related enhanced primary production has influences on the benthic realm in different ways. Foraminiferal diversities close to the ice edge were considerably affected by ice-edge-related high phytoplankton sedimentations, acting like a natural disturbance event. Following the latitudinal gradient in food supply, foraminiferal diversities increase again significantly. But ultimately, coupled with the further decreasing availability of fresh organic matter, the diversities again decrease.

References

Altenbach AV (1992) Short term processes and patterns in the foraminiferal response to organic flux rates. Mar Micropaleontol 19:119–129

Barnett PRO, Watson J, Conelly D (1984) A multiple corer for taking virtually undisturbed samples from shelf, bathyal and abyssal sediments. Oceanol Acta 7:399–408

Billett DSM, Lampitt RS, Rice AL (1983) Seasonal sedimentation of phytoplankton to the deep-sea benthos. Nature 302:520–522

Boetius A, Damm E (1998) Benthic oxygen uptake, hydrolytic potentials and microbial biomass at the Arctic continental slope. Deep Sea Res 45:239–275

Boetius A, Lochte K (1994) Regulation of microbial enzymatic degradation of OM in deep-sea sediments. Mar Ecol Prog Ser 104:299–307

Boetius A, Lochte K (1996) Effect of organic enrichments on hydrolytic potentials and growth of bacteria in deep-sea sediments. Mar Ecol Prog Ser 140:239–250

Børsheim KY, Bratbak G, Heldal M (1990) Enumeration and biomass estimation of planktonic bacteria and viruses by transmission electron microscopy. Appl Environ Microbiol 56:352–356

Caswell H (1976) Community structure: a neutral model analysis. Ecol Monogr 46:327–354

Connell JH (1978) Diversity in tropical forests and coral reefs. Science 199:1302–1310

Corliss BH, Emerson S (1990) Distribution of Rose Bengal stained deep-sea benthic Foraminifera from the Nova Scotian continental margin and Gulf of Maine. Deep Sea Res 37:381–400

Cota GF, Legendre L, Gosselin M, Ingram RG (1991) Ecology of bottom ice algae. I. Environmental controls and variability. J Mar Syst 2:257–277

Ewens WJ (1972) The sampling theory of selectively neutral alleles. Theor Popul Biol 3:87–112

Falk-Petersen S, Hop H, Budgell WP, Hegseth EN, Korsnes R, Loeyning TB, Oerbaek JB, Kawamura T, Shirasawa K (2000) Physical and ecological processes in the marginal ice zone of the northern Barents Sea during the summer melt period. J Mar Syst 27:131–159

Findlay RH, Dobbs FC (1993) Quantitative description of microbial communities using lipid analysis. In: Kemp PF, Sherr BF, Sher EB, Cole JJ (eds) Handbook of methods in aquatic microbial ecology. Lewis, Boca Raton, pp 271–284

Goldman N, Lambshead PJD (1989) Optimization of the Ewens/Caswell neutral model program for community diversity analysis. Mar Ecol Prog Ser 50:255–261

Gooday AJ (1994) The biology of deep-sea foraminifera: a review of some advances and their applications in paleooceanography. Palaios 9:14–31

Gooday AJ, Carstens M, Thiel H (1995) Micro- and nanoforaminifera from abyssal Northeast Atlantic Sediments: a preliminary report. Int Rev Ges Hydrobiol 80:361–383

Gooday AJ, Pfannkuche O, Lambshead PJD (1996) An apparent lack of response by metazoan meiofauna to phytodetritus deposition in the bathyal north-eastern Atlantic. J Mar Biol Assoc UK 76:297–310

Greiser N, Faubel A (1988) Biotic factors. In: Higgins RP, Thiel H (eds) Introduction to the study of meiofauna. Smithsonian Institution, Washington, DC, pp 79–114

Grossmann S, Reichhardt W (1991) Impact of *Arenicola Marina* on bacteria in intertidal sediments. Mar Ecol Prog Ser 77:85–93

Hurlbert SH (1984) Pseudoreplication and the design of ecological field experiments. Ecol Monogr 54:187–211

Huston M (1979) A general hypothesis of species diversity. Am Nat 113:81–101

Kaleschke L, Lüpkes C, Vihma T, Haarpaintner J, Bochert A, Heygster G (2001) SSM/I Sea ice remote sensing for mesoscale ocean-atmosphere interaction analysis. Can J Remote Sensing 27:526–532

Karl DM (1993) Total microbial biomass estimation derived from the measurement of particulate adenosine-5′-triphosphate. In: Kemp PF, Sherr BF, Sher EB, Cole JJ (eds) Handbook of methods in aquatic microbial ecology. Lewis, Boca Raton, pp 271–284

Lambshead PJD, Platt HM (1988) Analysing disturbance with the Ewens/Caswell neutral model: theoretical review and practical assessment. Mar Ecol Prog Ser 43:31–41

Manley TO (1995) Branching of Atlantic water within the Greenland-Spitsbergen Passage: an estimate of recirculation. J Geophys Res 100:20627–20634

Meyer-Reil L-A, Köster M (1992) Microbial life in pelagic sediments: the impact of environmental parameters on enzymatic degradation of organic material. Mar Ecol Prog Ser 81:65–72

Murray JL (1998) Physical/geographical characteristics of the Arctic. In: Wilson SJ, Murray JL, Huntington HP (eds) AMAP assessment report: Arctic pollution issues. Arctic Monitoring and Assessment Programme (AMAP), Oslo, pp 9–24

Pfannkuche O, Thiel H (1987) Meiobenthic stocks and benthic activity on the NE-Svalbard Shelf and in the Nansen Basin. Polar Biol 7:253–266

Platt HM, Lambshead PJD (1985) Neutral model analysis of patterns of marine benthic species diversity. Mar Ecol Prog Ser 24:75–81

Rajendran N, Matsuda O, Urushigawa Y (1992) Distribution of polarlipid fatty acid biomarkers for bacteria in sediments of a polluted bay. Microbios 72:143–152

Rudels B, Meyer R, Fahrbach E, Ivanov VV, Østerhus S, Quadfasel D, Schauer U, Tverberg V, Woodgate RA (2000) Water mass distribution in Fram Strait and over the Yermak Plateau in summer 1997. Ann Geophys 18:687–705

Sakshaug E, Skjoldal HR (1989) Life at the ice edge. Ambio 18:60–67

Sakshaug E, Slagstad D (1991) Light and productivity of phytoplankton in polar marine ecosystems: a physiological view. Polar Res 10:69–85

Schewe I (2001) Small-sized benthic organisms of the Alpha Ridge, central Arctic Ocean. Int Rev Ges Hydrobiol 86:317–335

Schewe I, Soltwedel T (1999) Deep-sea meiobenthos of the central Arctic Ocean: distribution patterns and size-structure under extreme oligotrophic conditions. Vie Milieu 49:79–92

Smart CW, Gooday AJ (1997) Recent benthic foraminifera in the abyssal Northeast Atlantic Ocean: relation to phytodetrital inputs. J Foraminiferal Res 27:85–92

Soltwedel T, Schewe I (1998) Activity and biomass of the small benthic biota under permanent ice-coverage in the central Arctic Ocean. Polar Biol 19:52–62

Soltwedel T, Mokievsky V, Schewe I (2000) Benthic activity and biomass on the Yermak Plateau and in adjacent deep-sea regions northwest of Svalbard. Deep Sea Res I 47:1716–1785

Subba Rao DV, Platt T (1984) Primary production of Arctic waters. Polar Biol 3:191–201

Thiel H (1978) Benthos in upwelling regions. In: Boje R, Tomczak M (eds) Upwelling ecosystems. Springer, Berlin Heidelberg New York, pp 124–138

Venrick EL (1971) The statistics of subsampling. Limnol Oceanogr 16:811–818

Walsh JJ, McRoy CP, Coachman LK, Goering JJ, Nihoul JJ, Whitledge TE, Blackburn TH, Parker PL, Wirick CD, Shuert PG, Grebmeier JM, Springer AM, Tripp RD, Hansell DA, Djendi S, Deleersnijder E, Herinksen K, Lund BA, Andersen P, MuK ller-Karger FE, Dean K (1998) Carbon and nitrogen cycling within the Bering/Chuchki Seas: source regions for organic matter electing AOU demands of the Arctic Ocean. Progr Oceanogr 22:277–359

Wollenburg JE, Kuhnt W (2000) The response of benthic foraminifers to carbon flux and primary production in the Arctic Ocean. Mar Micropaleontol 40:189–231